ANALYTICAL PERFORMANCE, LOADS, AND AEROELASTIC STABILITY OF A FULL-SCALE ISOLATED PROPROTOR

Sesi Kottapalli
Aeromechanics Office
NASA Ames Research Center
Moffett Field, California
sesi.b.kottapalli@nasa.gov

C. W. Acree, Jr.
Aeromechanics Office
NASA Ames Research Center
Moffett Field, California
cecil.w.acree@nasa.gov

The prediction of the performance and loads of a full-scale isolated proprotor and the calculation of whirl flutter stability of the rotor installed in a wind tunnel are considered in this study. The comprehensive analysis CAMRAD II is used. The test article is a research proprotor based on the AW609 rotor and the wind tunnel test apparatus is the newly developed Tiltrotor Test Rig (TTR) installed in the USAF NFAC 40- by 80-Foot Wind Tunnel. The performance and loads predictions and the stability calculations cover the following operating conditions: hover, airplane mode, conversion, and helicopter mode. These pre-test analytical results are being obtained to identify test operating limits, ensure a safe wind tunnel test, and predict test results. Performance and loads test results to date show that rotor torque and yoke lag moment may limit the test envelope. Stability analysis shows that the TTR/609 is solidly stable within the test envelope.

Notation

609	Research proprotor based on the AW609 rotor
JVX	Joint Vertical Experimental proprotor
NFAC	USAF National Full-Scale Aerodynamics Complex at NASA Ames Research Center
OARF	Outdoor Aerodynamic Research Facility
T	Rotor thrust, lb
TTR	Tiltrotor Test Rig
V	Wind tunnel airspeed, knots

Sign convention

Lag bending moment: + tip bent toward leading edge
Flap bending moment: + tip bent down
Pitch link load: + for tension
Torsion moment: + tip twisted leading edge up

Introduction

This study is being undertaken in order to provide pre-test analytical predictions for a full-scale isolated proprotor test in the USAF National Full-Scale Aerodynamics Complex (NFAC) 40- by 80-Foot Wind Tunnel at NASA Ames. The test article is a 3-bladed research rotor derived from the right-hand rotor of the AW609; in this paper, this research rotor is referred to as "609". The test is an integral part of the initial checkout test of the newly developed Tiltrotor Test Rig (Ref. 1), whose purpose is to test advanced, full-scale proprotors in the NFAC. Figure 1 shows the 609/TTR currently installed in the NFAC 40x80-foot test section. The TTR rotor axis is horizontal and the rig rotates in yaw on the wind tunnel turntable for conversion (transition) and helicopter mode testing.

The general TTR research areas in proprotor aeromechanics include:

- Performance and efficiency in hover, transition and forward flight
- Vibration and dynamic loads for all flight regimes
- Hub and control loads for all flight regimes
- Variable-frequency dynamics (wide RPM range)

The supporting research opportunities are: acoustics measurements, flow visualization, and tunnel blockage effects.

The TTR is capable of testing various rotor types: articulated, gimballed, soft in-plane and hingeless with rotor diameters up to 26 ft, the 40x80-foot test section limit for good data.

A wind tunnel test can safely collect data for operating conditions beyond an aircraft flight envelope. The TTR has a large excess of available power. With all of its four motors operating, the present TTR operational power range extends up to 5000 hp, which is far greater than that of the AW609 aircraft. Also, in flight, cruise thrust is much lower than in hover, so the wind tunnel thrust limits do not necessarily apply.

Presented at the AHS Technical Conference on Aeromechanics Design for Transformative Vertical Flight, San Francisco, CA, January 16-19, 2018.

This paper summarizes the analytical effort to identify test operating limits (609 rotor performance and loads) and predict test results; the 609/TTR whirl flutter stability is also considered in this study. Eventually, the goal is to perform a correlation study, identify shortfalls in the analytical model, and introduce improvements to the analytical model.

609 research rotor and Tiltrotor Test Rig

Brief descriptions of the 609 research rotor and the TTR are given below.

609 research rotor

The 609 rotor currently undergoing testing in the USAF NFAC 40- by 80-Foot Wind Tunnel is based on the AW609 rotor. The rotor was manufactured by Bell Helicopter under contract to NASA. The main differences between the research and flight rotors are listed below; the research rotor:

- Does not have deicing capability
- Has additional instrumentation
- Has a different pitch horn arrangement, specific to the TTR control system
- Does not have pendulum absorbers

The rotor has three blades with non-linear twist and square tips, the rotor diameter is 26 ft and the geometric solidity is 0.097. The rotor is stiff in-plane with a gimballed hub and yoke (flexbeam). The conversion and helicopter mode rpm is 569 (100%) and the airplane mode (cruise) rpm is 478 (84%).

Tiltrotor Test Rig (TTR)

As noted in the Introduction, the TTR rotor axis is horizontal and the rig rotates in yaw on the wind tunnel turntable for conversion (transition) and helicopter mode testing. An overview of the TTR test objectives and the current initial checkout test are given in Ref. 1 (TTR Overview Presentation) and outlined here.

The primary purpose of the ongoing checkout test is to demonstrate the operational capability of the TTR over a wide range of test conditions. A secondary goal is to safely collect as much research data as possible. The resulting power, speed and loads will be high because the wind tunnel operating conditions will be beyond the aircraft flight envelope; the use of an existing rotor, the 609, minimizes risk (Ref. 1, TTR Overview Presentation).

Generally, the TTR test objectives are to:

- Fill gaps in existing tilt-rotor experimental databases by testing for classic rotor performance, including:
    - Hover, up to and beyond stall
    - Axial flow beyond 200 knots (up to the 300-knot NFAC limit)
    - Helicopter and transition modes up to 150 knots (includes edgewise flight)
- Conduct extended testing beyond the aircraft flight envelope, such as:
    - Slowed rotor in cruise for efficiency (50-75% hover tip speed)
    - Slowed rotor in hover for low noise (85% tip speed)

Analytical Model

The rotorcraft comprehensive analysis CAMRAD II Release 4.9, Refs. 2-4, is used for the analytical predictions. Table 1 summarizes the analytical models used in this study for the performance and loads task and the stability task. The two tasks were executed separately (two sets of CAMRAD II runs). For consistency, the trim procedure was kept the same in both tasks. Performance and loads calculations are being performed for the 609 rotor with flexible blades and hub, including the gimbal, but with no fixed system flexibility. For stability calculations, the fixed system dynamics are represented by experimentally determined modes (Ref. 5) and NASTRAN modes.

609 rotor model

The most recent CAMRAD II structural model for the 609 rotor/hub/blade is used in this study. Similar to the V-22 CAMRAD model (Ref. 6), a dual load-path model is used for the 609 rotor. The yoke (flexbeam) and the blade form the two load paths. The CAMRAD II aerodynamic model requires airfoil tables and these were provided by Bell Helicopter as C81 tables. For the performance and loads predictions the CAMRAD II rolled up wake model was used, and for the stability analyses the uniform inflow model was used.

The rotor model includes the gimbal and swashplate degrees of freedom, Table 1. In the trim calculations, for both tasks (performance and loads and stability), 12 elastic blade modes were used (torsion, flap and lag); for stability analyses, 8 elastic blade modes were used.

Airframe (TTR) model

Three orientations of the TTR were considered for the stability task:

- 0-deg yaw (airplane mode)
- 45-deg yaw (conversion)
- 90-deg yaw (helicopter mode)

The 0-deg yaw condition involves the highest airspeeds and is the most important condition for stability.

For the TTR installed in the NFAC 40x80-foot test section, shake test modal data are available, Ref. 5. These experimental modal data are used in the current study. A

NASTRAN model of the TTR was used for design and preliminary evaluations of TTR/609 stability. That model is being updated to include findings of the shake test and will be considered for further analyses. In contrast, all results reported herein are based strictly on experimentally determined mode shapes, frequencies, and damping.

The current stability analyses (based on shake test data) use 8 elastic TTR modes for the 0-deg yaw airplane condition and 7 elastic TTR modes for the 45-deg yaw conversion and the 90-deg yaw helicopter conditions. Tables 2a-2d list the TTR mode frequencies and damping for the above TTR orientations. For the 90-deg orientation, two sets of experimental modal data (from rap test and shake test, Tables 2c-2d) were available for analysis. The TTR mode "Nose Yaw" involving lateral motion of the TTR nose has the lowest frequency (approximately 2 Hz, Tables 2a-2d) and is the most important mode for whirl flutter stability.

Results

Analytical performance and loads predictions for the 609 rotor and stability calculations for the 609/TTR installed in the 40x80 wind tunnel are being performed in this ongoing study. Representative results are shown in this paper. Specifically, these include:

- Reality checks
- Performance and loads predictions, outlined in Table 3. Table 3 shows all cases to date, with variations in operating condition, associated flow condition, rpm, yaw (nacelle angle), and airspeed (all cases include thrust sweeps). The operating conditions include hover, cruise (airplane mode), conversion and helicopter mode at various yaw angles. Points outside the AW609 conversion corridor are included (Fig. 2). The approximate conversion corridor shown in Fig. 2 is derived from Refs. 7 and 9. The Fig. 2 analysis points, specific to the current wind tunnel test, are not necessarily applicable to the aircraft in flight.
- Stability predictions for hover, airplane (0-deg yaw, and conversion and helicopter modes (45-deg and 90-deg yaw, respectively).

Reality checks

Prior to the production running of the large number of the required pre-test CAMRAD II performance and loads cases, reality checks were made to ensure the predicted numbers are in reasonable range. As background, the JVX rotor is closely similar to the 609 in size and aerodynamics, and is accordingly a good reference for performance calculations (Ref. 8 contains more information on the JVX rotor). Reality checks were made by comparing JVX and 609 predictions in hover and forward flight (airplane mode). The figure of merit is chosen for the hover comparison as this performance parameter is more sensitive to small changes compared to, for example, the power coefficient. As a first check of the analytical model, Fig. 3a (Ref. 8) shows correlation for the JVX only – the correlation is excellent. In Fig. 3a, "3 trailers" refers to the wake model used in Ref. 8. Figure 3b compares the predicted figures of merit for the JVX and 609 – the takeaway from this figure is that the 609 prediction looks reasonable.

For forward flight, Fig. 4a shows the Ref. 8 correlation for JVX power (wind tunnel data) – this correlation is also excellent. In Ref. 8, all JVX data at advance ratio=0.523 and below were taken at 487 rpm, but the data at advance ratio=0.562 were taken at 531 rpm. Note that the JVX and 609 rotor radii are slightly different (12.5 ft and 13.0 ft, respectively). For comparing JVX performance with that of the 609, the advance ratios were matched exactly and all 609 results were obtained at the cruise rpm of the 609 (478 rpm). A 609 CAMRAD II run was made for advance ratio=0.562 with rpm=531; no significant difference was found with the corresponding results at rpm=478. Thus, for current purpose, matching advance ratios is sufficient. Figure 4b compares the predicted power for the JVX and 609, and the takeaway from this figure is that the 609 predictions look reasonable; given that the two rotors are slightly different, it is not surprising that the predictions are also slightly different. To sum it up, the current hover and forward flight comparisons look reasonable thus lending confidence in the analytical model.

Representative performance and loads

Figure 5a-5c show the hover thrust, torque and pitch link load vs. collective (blade pitch at 0.75R) at 569 rpm. As a reality check, also included are recently acquired "checkout" test data points for the 609/TTR in the wind tunnel. The checkout test points were obtained during initial TTR track and balance runs and are not necessarily representative of typical rotor behavior. Nevertheless, the near match between predictions and data is encouraging. For current purposes, the agreement between the predictions and measurements is reasonable. For the thrust and torque, Figs. 5a-5b, the TTR/609 test limits are also shown; these represent static design load limits. Note that in Fig. 5b, which shows the torque variation, the equivalent power limit is also shown.

Figures 6a-6f show the cruise thrust, torque, pitch link load, and yoke (flexbeam) torsion, flap and lag moments at 250 knots airspeed and 478 rpm. Where applicable, Figs. 6a-6f also show the TTR/609 test limits; for the thrust, torque, and pitch link load these test limits represent static design load limits. For the yoke (flexbeam) flap and lag moments, the TTR/609 test limits represent "alerts" which correspond to roughly 80%-90% of the design loads. The results show that the test envelope may be limited by the torque, Fig. 6b.

Figures 7a-7g show the conversion thrust, torque, pitch link load, yoke (flexbeam) torsion, flap and lag moments, and trim cyclics for 45-deg yaw, 125 knots airspeed and 569 rpm. Mean, max and min quantities (± ½ peak-to-peak) are shown where relevant. The TTR/609 test limits that have been described earlier (cruise - Figs. 6a-6f) are also applicable to the conversion results, Figs. 7a-7f. For the trim cyclics shown in Fig. 7g, the TTR/609 test limits are based on the 609 gimbal angle limits. The rotor was trimmed to specified thrust and zero 1P flapping. The results show that the test envelope may be limited by the torque and possibly the yoke minimum lag moment.

The load limits of Figs. 5b, 6b, 7b, and 7f are reached at very high power. In the wind tunnel, the 609 will be operated at power levels in excess of aircraft power in flight. Therefore, the load limits predicted here do not necessarily represent limitations on the 609 aircraft.

Stability

Figures 8a-8b show hover damping and frequency variations vs. C_T/σ, 569 rpm. The rotor is completely stable up to C_T/σ=0.2, which approximately equals 15,000 lb thrust and requires 2719 hp. In the current checkout test, the TTR is being operated with two motors – the power limit is 2500 hp. Hover stability is therefore of no concern for the TTR/609 with only two motors operating.

Figures 9a-9b show cruise (airplane mode, axial flow) damping and frequency variations vs. airspeed for zero power, 478 rpm (zero power is the worst case for whirl flutter for a gimballed rotor with precone). Figure 9a shows that the TTR/609 in the NFAC 40x80 wind tunnel is stable with > 1% critical damping for airspeeds < 300 knots (the maximum wind tunnel airspeed). The critical mode for stability is the nose yaw mode, which involves lateral bending of the forward support strut (Fig. 1). This mode is specific to the TTR as installed in the 40- by 80-ft test section. See Ref. 9 for a discussion of aeroelastic stability of the actual aircraft.

For conversion and helicopter mode conditions that involve edgewise and axial flow, the 609 rotor was trimmed to specified thrust and zero 1P flapping. The following sets of shake test data are available for conversion and helicopter mode conditions: for 45-deg TTR yaw, rap test data are available and for 90-deg TTR yaw, both rap test and shake test data are available, Ref. 5. Hence, this paper presents the results of three stability analyses: 45-deg yaw with rap test data and 90-deg yaw with rap test and shake test data. It is to be noted that for conversion and helicopter mode conditions, the wind tunnel test envelope is restricted to airspeeds less than 150 knots based on TTR strut load limits.

For 45-deg yaw, Figs. 10a-10d show the trim quantities (thrust, resulting torque, and lateral and longitudinal cyclics) vs. airspeed (569 rpm). Figure 10a shows the eight trimmed thrust values for which the stability calculations were performed. The resulting torque values are shown in Fig. 10b along with the TTR/609 test limit (static design load limit). For the trim cyclics shown in Figs. 10c-10d, the lower and upper limits are also shown; as noted earlier, these TTR/609 test limits are based on the 609 gimbal angle limits. For these analyses, the rotor is being pushed well outside of the aircraft flight envelope (Fig. 2). The trimmed values of torque and cyclic in Figs. 10b-10d therefore represent values not always reachable in flight. Fig. 10e shows the 45-deg yaw stability envelope (rap test data based) for 1% critical damping. The Fig. 10e stability envelope shows that the TTR/609 is predicted to be stable (damping ≥ 1% critical) within the test envelope for thrust values smaller or equal to 8000 lb; for 10,000 lb thrust, comparable stability is obtained up to 100 knots.

Figures 11a-11c show the 90-deg yaw helicopter mode stability envelopes (569 rpm). Figure 11a shows the rap test data based 1% critical damping envelope and Figs. 11b and 11c show the corresponding shake test data based envelopes for 1% and 0.9% critical damping, respectively. Clearly, the two sets of test data (rap and shake test) result in roughly similar stability envelopes as can be seen from Figs. 11a and 11c. Specifically, Fig. 11a (rap test data based) shows that the TTR/609 is predicted to be stable (damping ≥ 1% critical) within the test envelope for thrust values smaller or equal to 9000 lb; for 10,000 lb thrust, comparable stability is obtained up to 120 knots. Also, Fig. 11c (shake test data based) shows that the TTR/609 is predicted to be stable (damping ≥ 0.9% critical) within the test envelope for thrust values smaller or equal to 9000 lb; for 10,000 lb thrust, comparable stability is obtained up to 90 knots.

The current stability predictions (hover, cruise, conversion, and helicopter mode) show that the TTR/609 is solidly stable within the test envelope.

Conclusions

Pre-test performance, loads and stability predictions for the isolated 609 rotor were considered in this ongoing analytical study. Performance and loads calculations were performed for the 609 rotor with flexible blades and hub, including the gimbal, but with no fixed system flexibility. For stability calculations, the fixed system dynamics were represented by mode shapes and frequencies experimentally determined by a shake test of the Tiltrotor Test Rig (TTR) installed in the USAF NFAC 40- by 80-Foot Wind Tunnel. All anticipated test conditions were covered in the analysis: hover, cruise (airplane mode), conversion and helicopter mode. These pre-test analytical results are being obtained to identify test operating limits, ensure a safe wind tunnel test, and predict test results. Specific conclusions from this analytical study are as follows:

1. Performance and loads results show that for some test conditions, the rotor torque, the yoke minimum lag moment, and the longitudinal cyclic may limit the test envelope. In the wind tunnel, the 609 will be operated at power levels in excess of aircraft power in flight. Therefore, the load limits predicted here do not necessarily represent limitations on the 609 aircraft.

2. Shake test data based stability calculations predict that the TTR/609 is solidly stable within the test envelope. The limiting mode is a strut mode specific to the NFAC installation; this limitation does not apply to the AW609 aircraft itself.

References

1. Tiltrotor Test Rig, Aeromechanics Office, NASA Ames Research Center, https://rotorcraft.arc.nasa.gov/Research/Facilities/ttr.html

2. Johnson, W., "CAMRAD II, Comprehensive Analytical Model of Rotorcraft Aerodynamics and Dynamics," Johnson Aeronautics, Palo Alto, California, 1992-1999.

3. Johnson, W., "Technology Drivers in the Development of CAMRAD II," American Helicopter Society, American Helicopter Society Aeromechanics Specialists Conference, San Francisco, CA, January 19-21, 1994.

4. Johnson, W., "A General Free Wake Geometry Calculation for Wings and Rotors," American Helicopter Society 51st Annual Forum Proceedings, Ft. Worth, TX, May 9-11, 1995.

5. Russell, C.R. and Acree, C.W., "Modal Test and Analysis of the NASA Tiltrotor Test Rig," to be presented at the American Helicopter Society Technical Conference on Aeromechanics Design for Transformative Vertical Lift, San Francisco, CA, January 16-19, 2018.

6. Acree, C. W. Jr., "A CAMRAD II Model of the V-22 Rotor for Whirl-Flutter Analysis", NASA TM 2004-212801, July 2004.

7. Harris, J.C., Scheidler, P.F, Hopkins, R, and Fortenbaugh, R.L., "Initial Power-Off Testing of the BA609 Tiltrotor," American Helicopter Society 66th Annual Forum Proceedings, Phoenix, AZ, May 11-13, 2010.

8. Acree, C.W., "JVX Proprotor Performance Calculations and Comparisons with Hover and Airplane-Mode Test Data", NASA/TM–2009-215380, April 2009.

9. Parham, T. and Corso, L. M., "Aeroelastic and Aeroservoelastic Stability of the BA 609," 25th European Rotorcraft Forum, September 1999.

Table 1. Summary of analytical models.

	Analysis task		
	Performance & loads	Stability	
		Trim	Flutter
Rotor			
Gimbal	Yes	Yes	Yes
Swashplate	Yes	Yes	Yes
Blade			
Torsion, flap, lag			
Total # of modes per blade	12	12	8
Airframe (TTR)			
Drive train, elastic	No	No	Yes
Elastic modes, shake test	No	No	7[a], 8[b]
Elastic modes, NASTRAN	No	No	15

[a] 7 TTR modes for conversion (45-deg yaw) and helicopter (90-deg yaw) conditions
[b] 8 TTR modes for airplane (cruise, 0-deg yaw) condition

Table 2a. TTR mode frequency and damping, 0-deg yaw, shake test data (Ref. 5).

	Mode	Frequency Hz	Structural damping (2*critical)
1.	Yaw mode about aft struts ("Nose Yaw")	1.97	0.0593
2.	Longitudinal strut mode ("RB Axial")	2.58	0.0185
3.	Yaw mode about fwd strut ("CG Yaw")	2.59	0.0296
4.	Vertical balance frame	8.40	0.0290
5.	TTR + balance frame pitch	11.37	0.0167
6.	Lateral shaft bending	14.80	0.0169
7.	Vertical shaft + TTR bending	15.31	0.0413
8.	TTR + vertical shaft bending	17.07	0.0244

Table 2b. TTR mode frequency and damping, 45-deg yaw, rap test data (Ref. 5).

	Mode	Frequency Hz	Structural damping (2*critical)
1.	Yaw mode about aft struts	2.05	0.0239
2.	Longitudinal strut mode	2.59	0.0235
3.	Yaw mode about fwd strut	2.94	0.0391
4.	Vertical balance frame	8.25	0.0554
5.	TTR + balance frame pitch	11.43	0.0181
6.	Lateral shaft bending	14.88	0.0206
7.	Vertical shaft + TTR bending	14.90	0.0281

Table 2c. TTR mode frequency and damping, 90-deg yaw, rap test data (Ref. 5).

	Mode	Frequency Hz	Structural damping (2*critical)
1.	Yaw mode about aft struts	2.06	0.0268
2.	Longitudinal strut mode	2.52	0.0230
3.	Yaw mode about fwd strut	2.79	0.0505
4.	Vertical balance frame	8.40	0.0415
5.	TTR + balance frame pitch	11.47	0.0200
6.	Lateral shaft bending	14.94	0.0179
7.	Vertical shaft + TTR bending	14.72	0.0231

Table 2d. TTR mode frequency and damping, 90-deg yaw, shake test data (Ref. 5).

	Mode	Frequency Hz	Structural damping (2*critical)
1.	Yaw mode about aft struts	1.99	0.0507
2.	Longitudinal strut mode	2.48	0.0231
3.	Yaw mode about fwd strut	2.47	0.0964
4.	Vertical balance frame	8.31	0.0184
5.	TTR + balance frame pitch	11.37	0.0176
6.	Lateral shaft bending	14.76	0.0167
7.	Vertical shaft + TTR bending	14.60	0.0236

Table 3. 609 rotor operating conditions for performance and loads predictions (includes thrust sweeps).

Operating condition	Flow condition	rpm	Yaw, deg (nacelle angle)	Airspeed knots
Hover	Axial	478, 569	90	0
Helicopter	Axial & edgewise	569	95	70
Helicopter	"	569	90	50, 90
Conversion	Axial & edgewise	569	85	50
"	"	569	75	70, 120
"	"	569	60	60, 100, 150
"	"	569	45	85, 125, 165
"	"	569	30	95, 140, 190
Conversion	Axial & edgewise	569	15	110, 165, 215
Cruise	Axial	478, 569	0	50
"	"	478, 569	0	100
"	"	478, 569	0	150
"	"	478, 569	0	200
"	"	478, 569	0	250
Cruise	Axial	478, 569	0	300

Fig. 1. TTR/609 installed in the USAF National Full-Scale Aerodynamics Complex (NFAC) 40x80-foot test section.

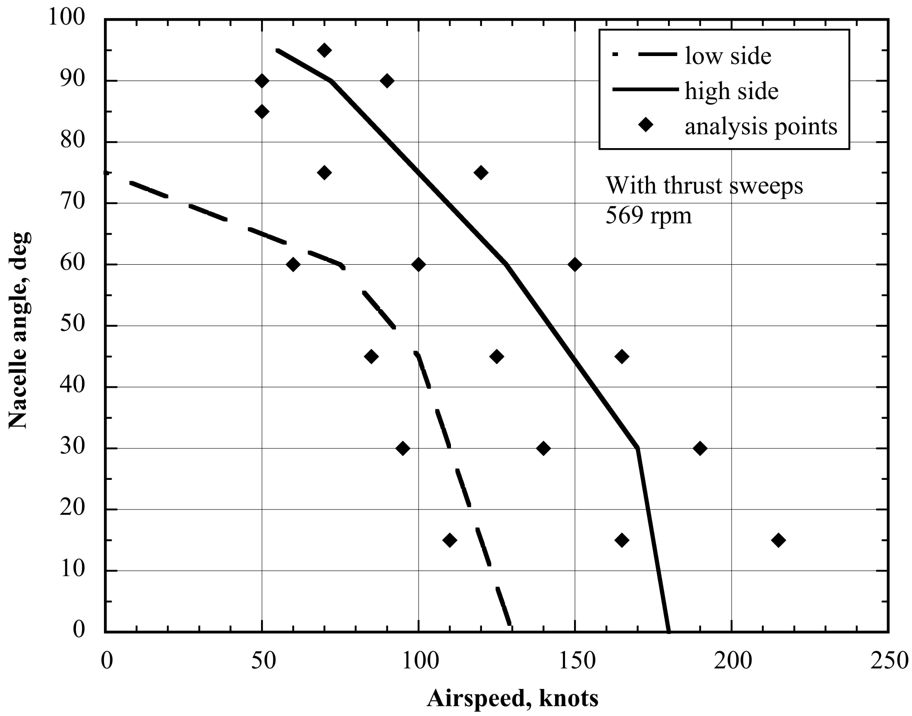

Fig. 2. Approximate AW609 conversion corridor (Refs. 7 and 9) and current pre-test 609 rotor analysis points, 569 rpm.

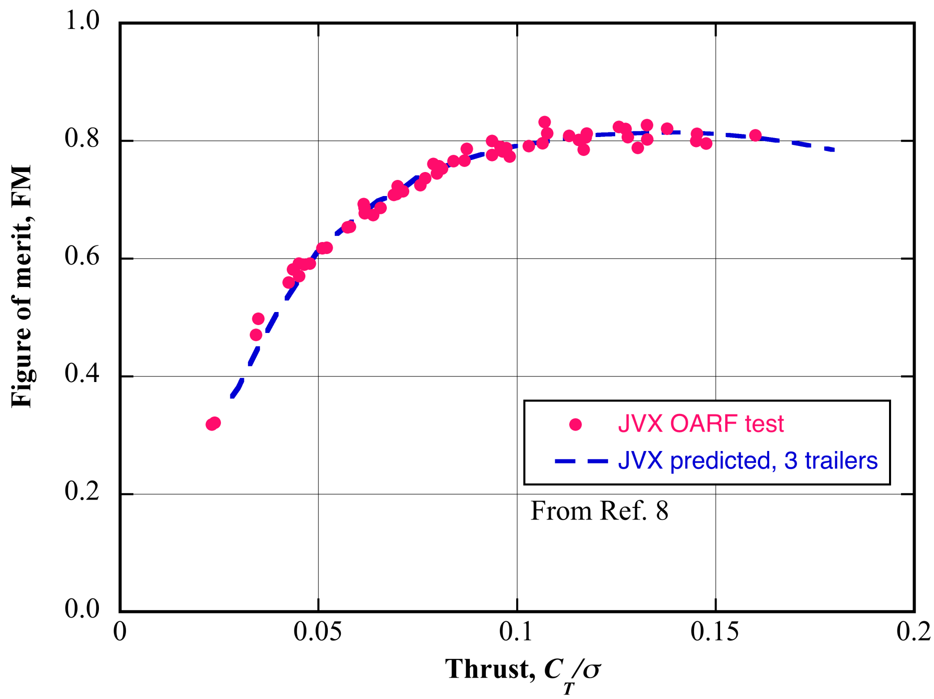

Fig. 3a. JVX figure of merit correlation (Ref 8).

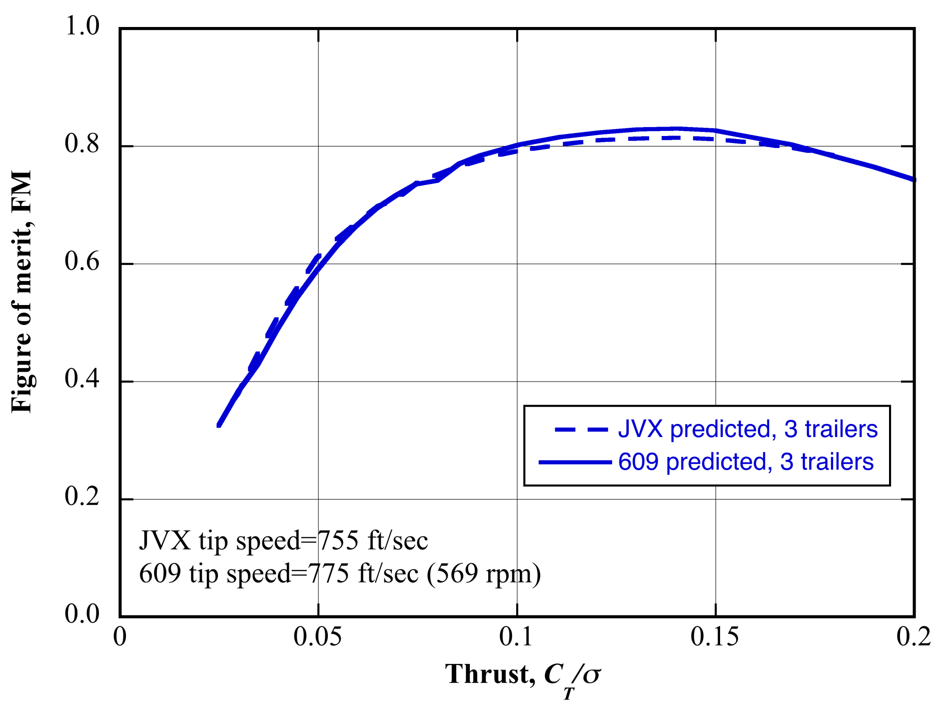

Fig. 3b. Reality check, JVX and 609 predicted figure of merit comparison (based on Ref 8).

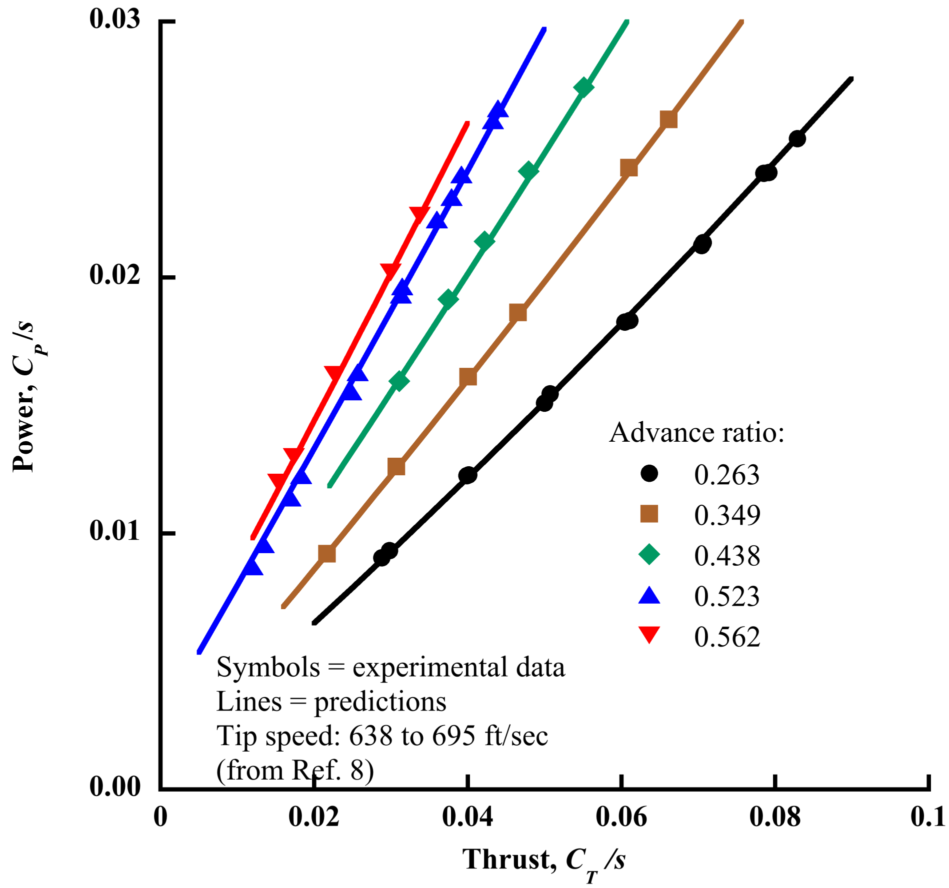

Fig. 4a. JVX forward flight power correlation (Ref. 8).

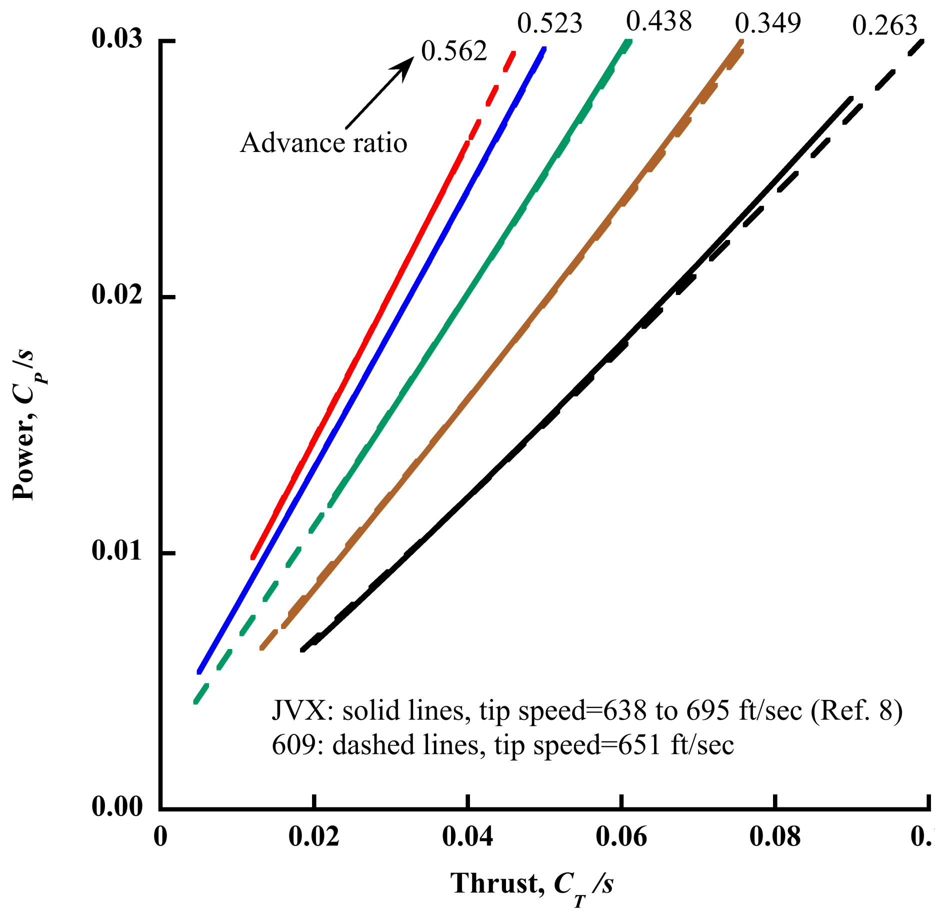

Fig. 4b. Reality check, JVX and 609 predicted forward flight power comparison.

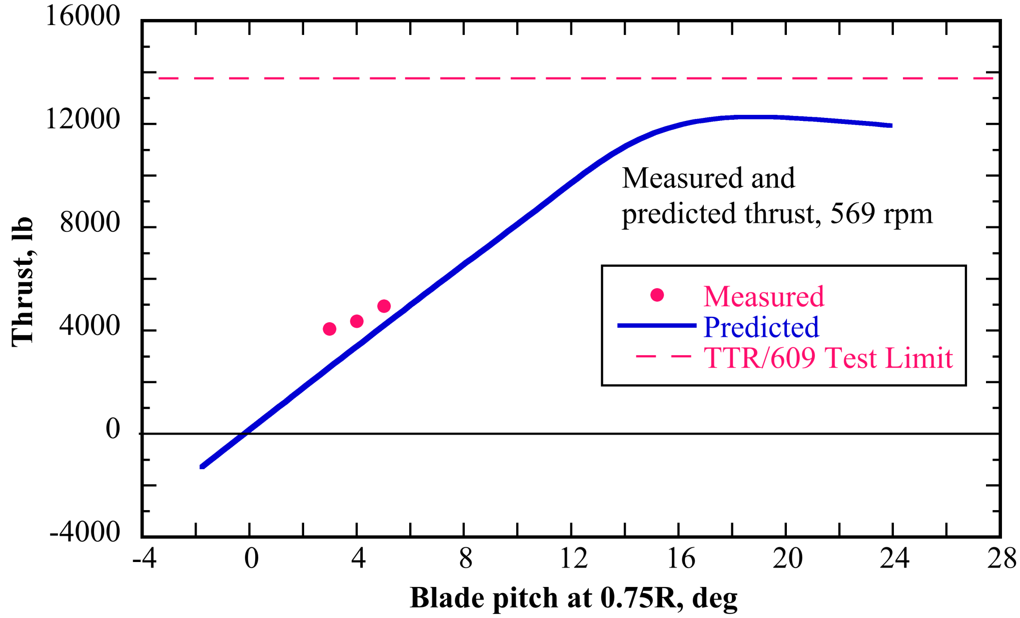

Fig. 5a. 609 hover thrust vs. collective, 569 rpm.

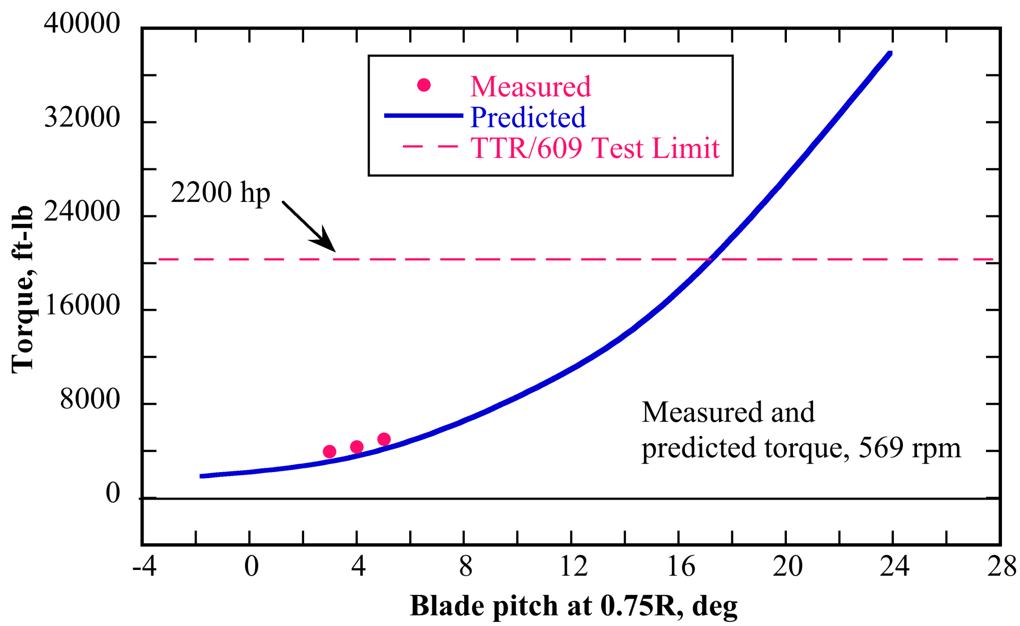

Fig. 5b. 609 hover torque vs. collective, 569 rpm.

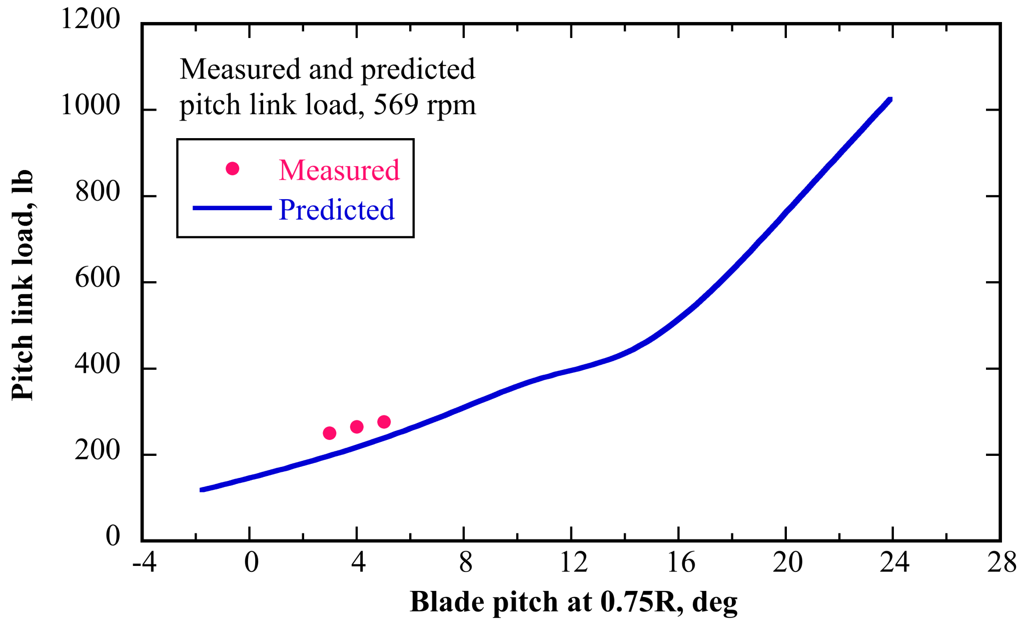

Fig. 5c. 609 hover pitch link load vs. collective, 569 rpm.

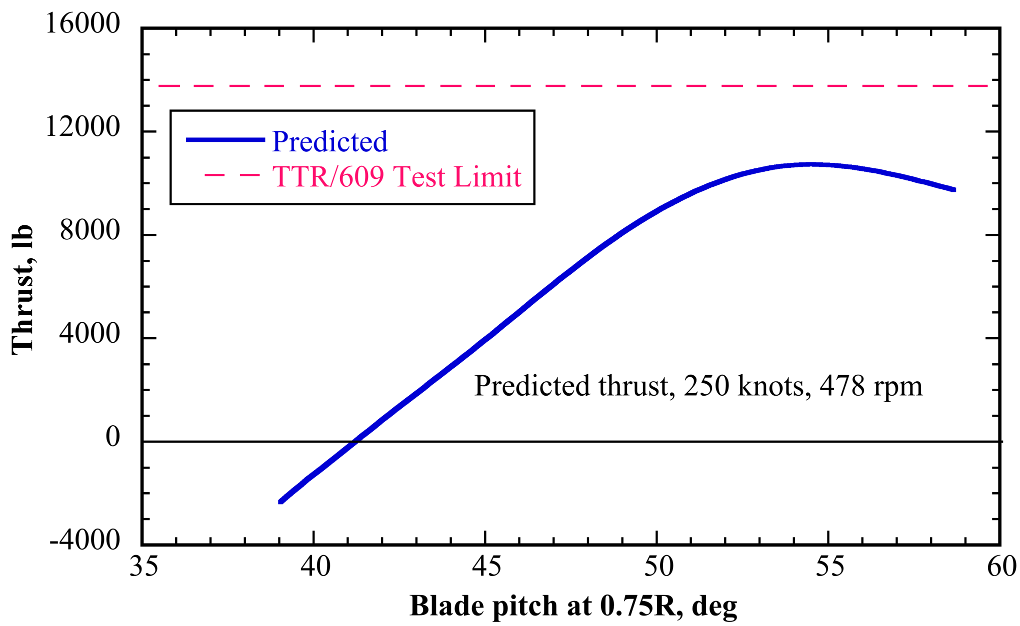

Fig. 6a. Predicted 609 cruise (axial flow) thrust vs. collective, 0-deg yaw, 250 knots, 478 rpm.

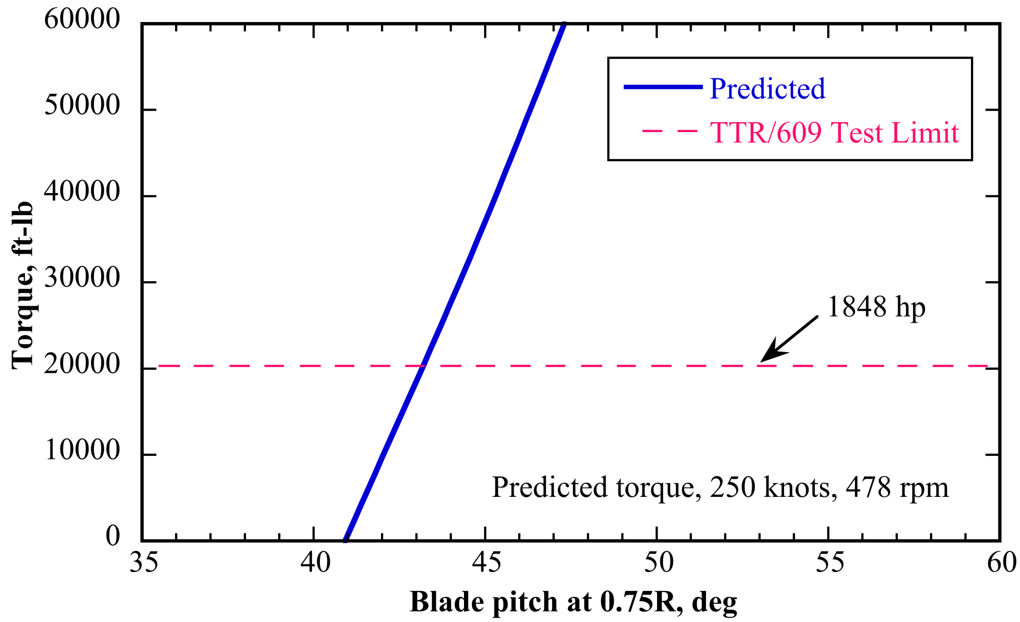

Fig. 6b. Predicted 609 cruise (axial flow) torque vs. collective, 0-deg yaw, 250 knots, 478 rpm.

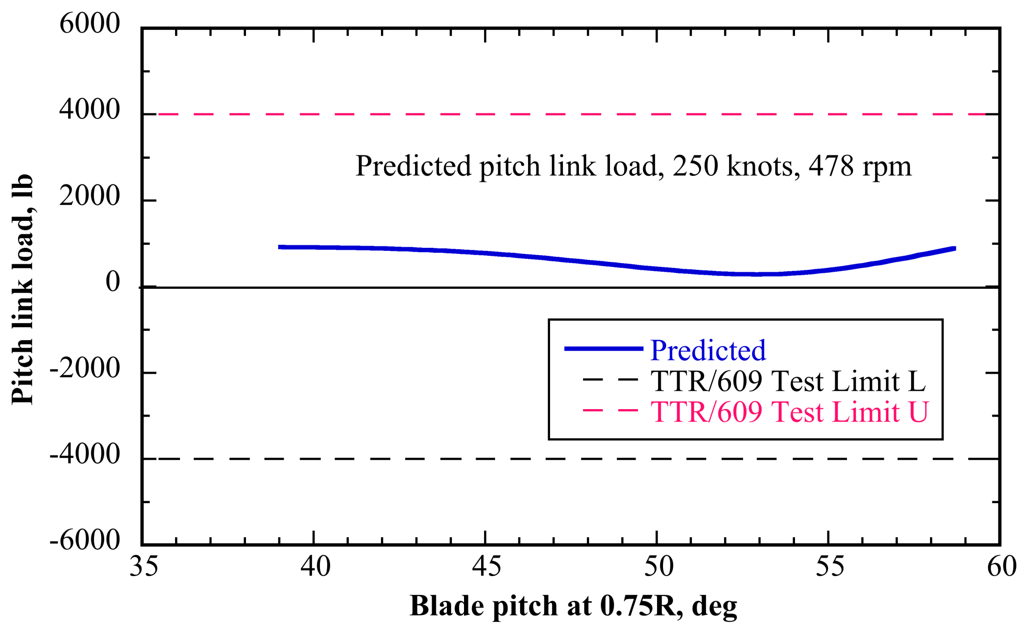

Fig. 6c. Predicted 609 cruise (axial flow) pitch link load vs. collective, 0-deg yaw, 250 knots, 478 rpm.

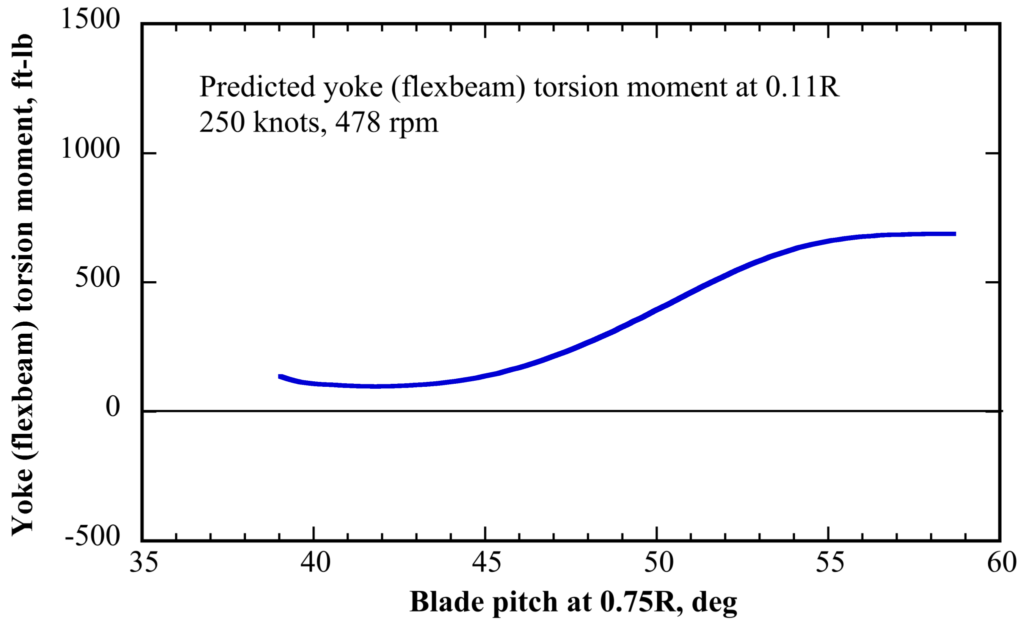

Fig. 6d. Predicted 609 cruise (axial flow) yoke torsion moment vs. collective, 0-deg yaw, 250 knots, 478 rpm.

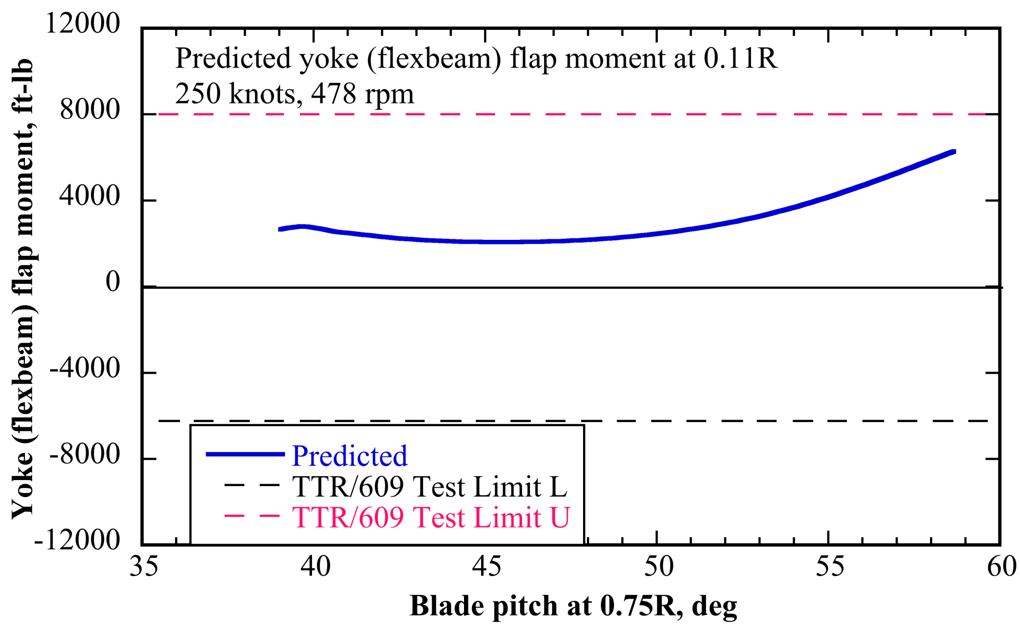

Fig. 6e. Predicted 609 cruise (axial flow) yoke flap moment vs. collective, 0-deg yaw, 250 knots, 478 rpm.

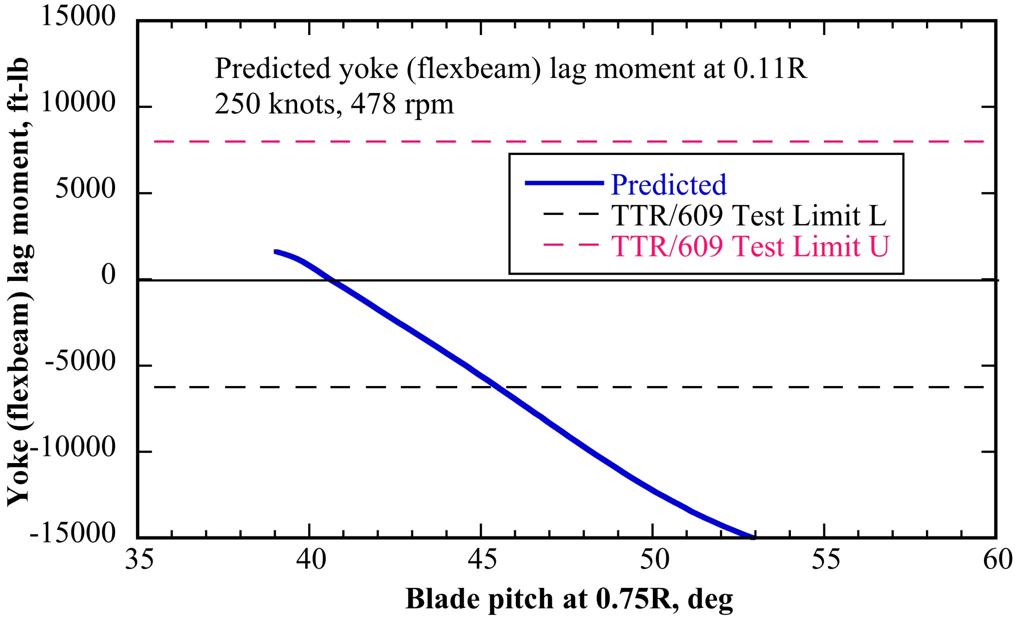

Fig. 6f. Predicted 609 cruise (axial flow) yoke lag moment vs. collective, 0-deg yaw, 250 knots, 478 rpm.

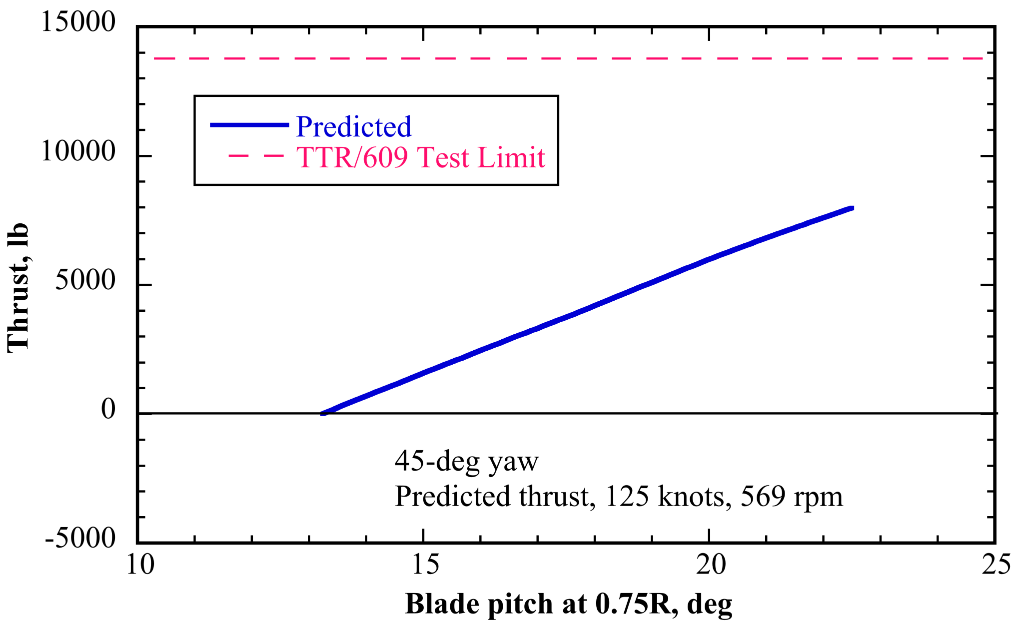

Fig. 7a. Predicted 609 conversion (axial and edgewise flow) thrust vs. collective, 45-deg yaw, 125 knots, 569 rpm.

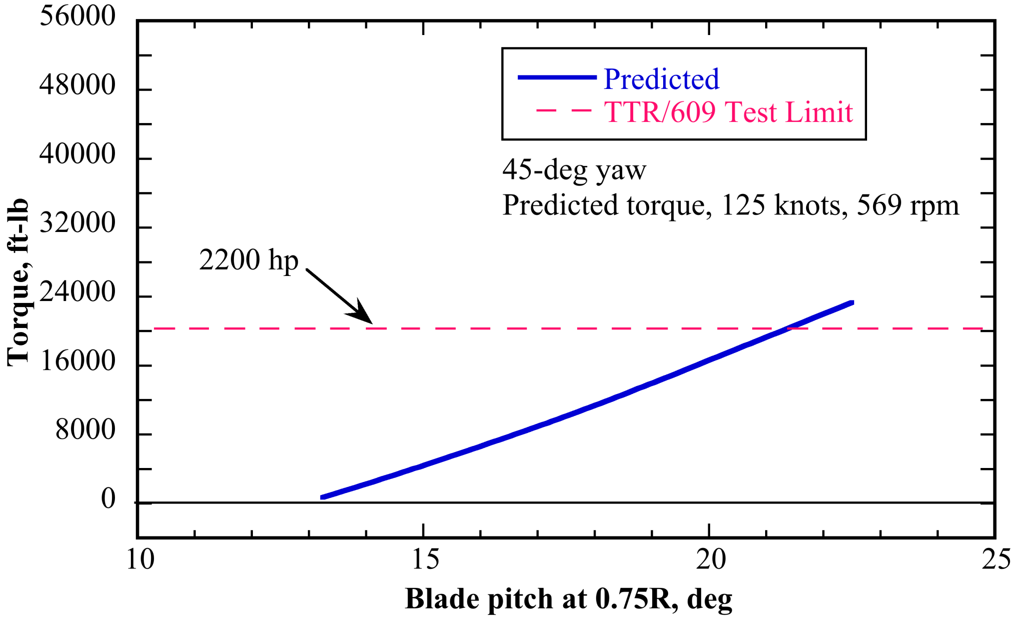

Fig. 7b. Predicted 609 conversion (axial and edgewise flow) torque vs. collective, 45-deg yaw, 125 knots, 569 rpm.

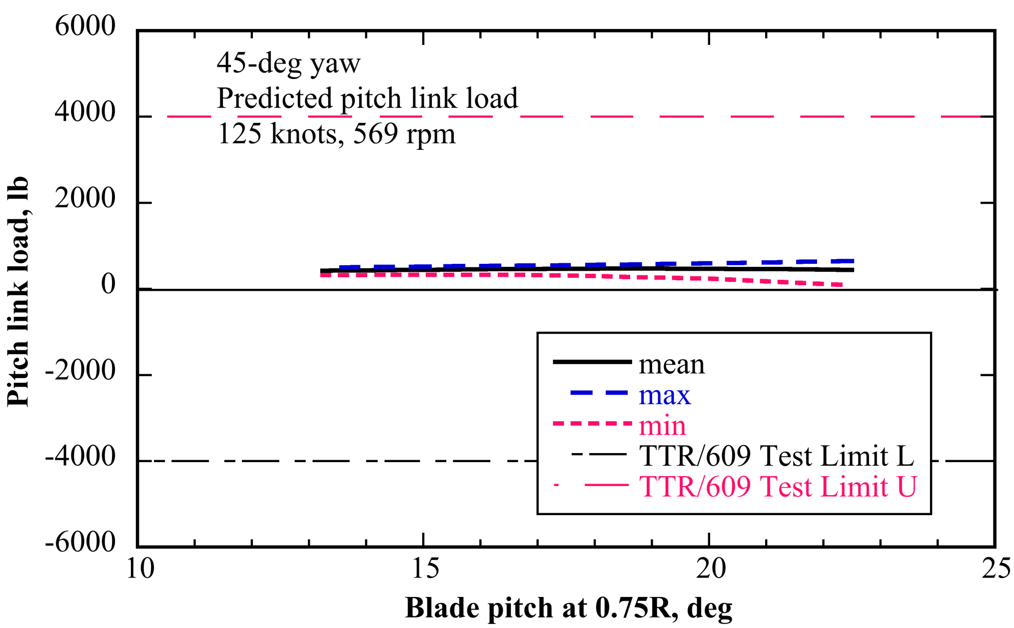

Fig. 7c. Predicted 609 conversion (axial and edgewise flow) pitch link load vs. collective, 45-deg yaw, 125 knots, 569 rpm.

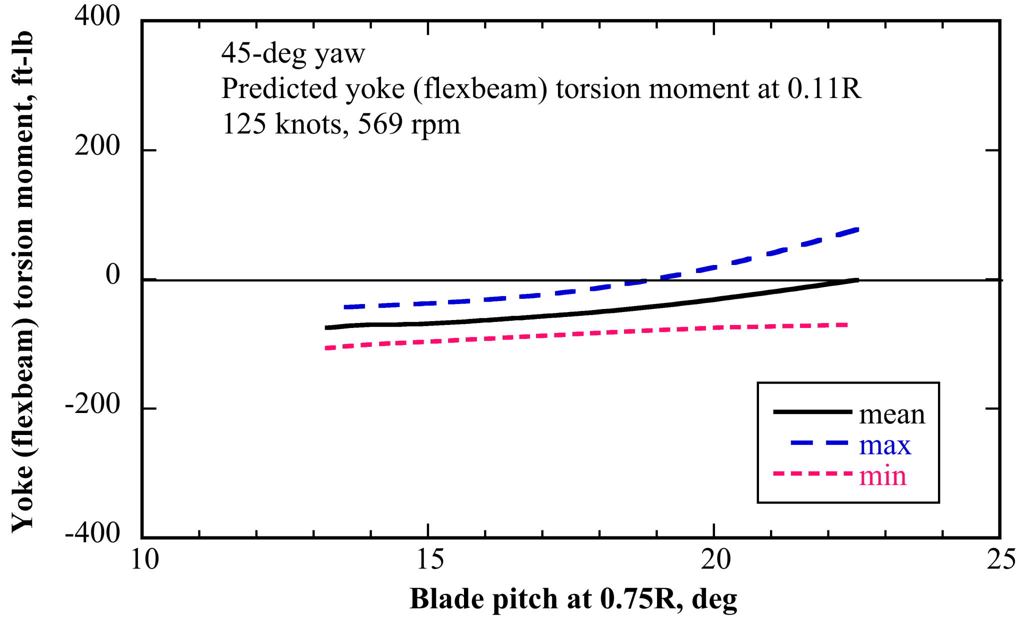

Fig. 7d. Predicted 609 conversion (axial and edgewise flow) yoke torsion moment vs. collective, 45-deg yaw, 125 knots, 569 rpm.

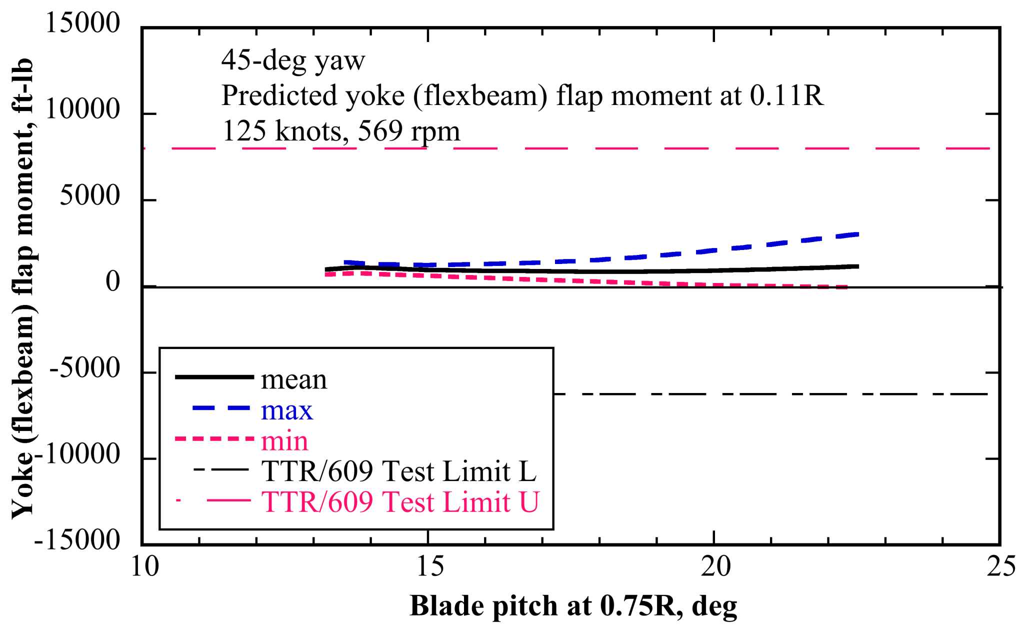

Fig. 7e. Predicted 609 conversion (axial and edgewise flow) yoke flap moment vs. collective, 45-deg yaw, 125 knots, 569 rpm.

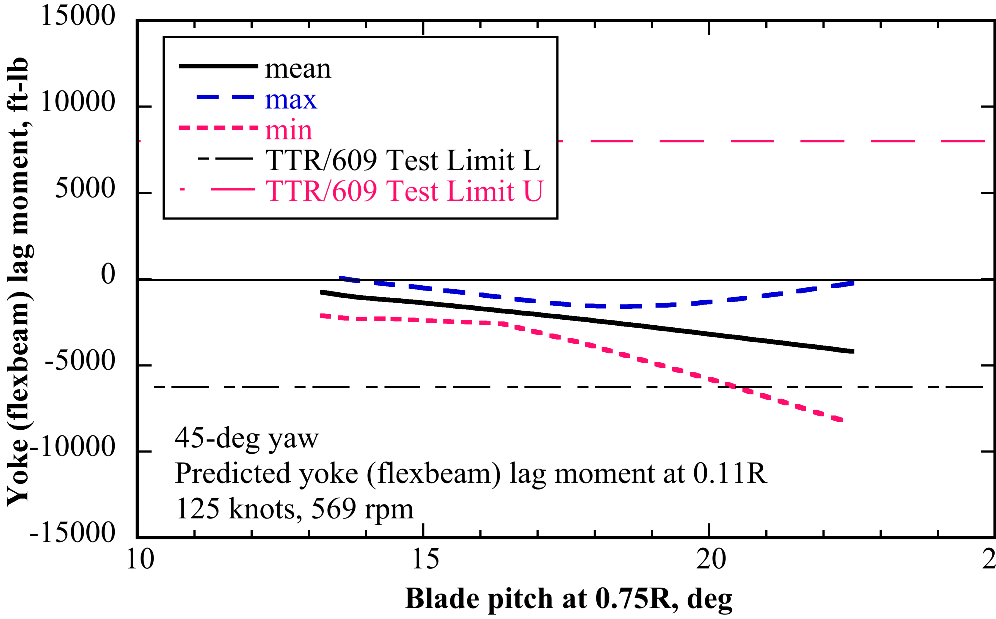

Fig. 7f. Predicted 609 conversion (axial and edgewise flow) yoke lag moment vs. collective, 45-deg yaw, 125 knots, 569 rpm.

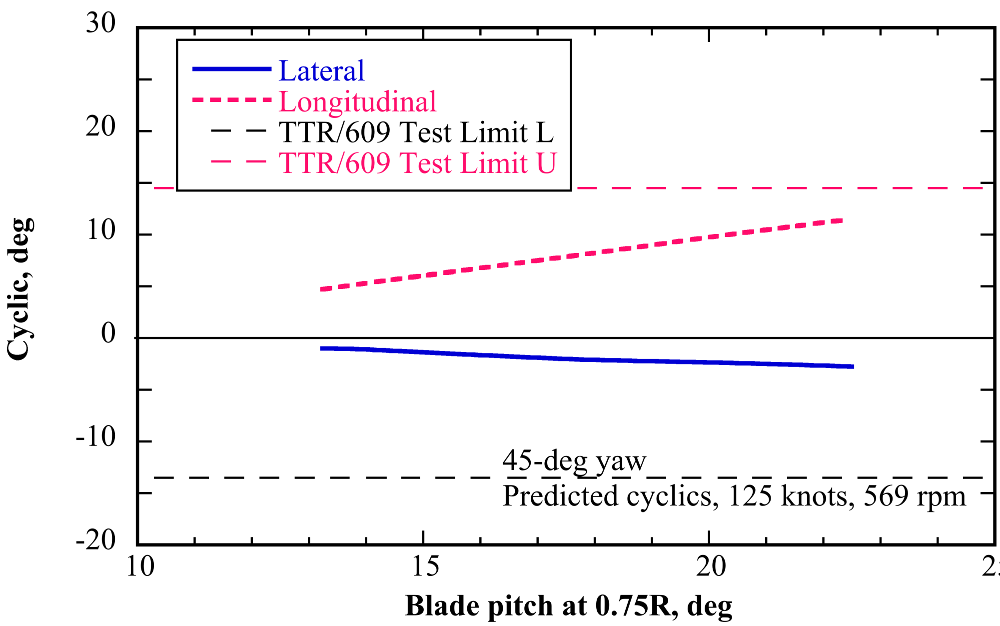

Fig. 7g. Predicted 609 conversion (axial and edgewise flow) trim cyclics vs. collective, 45-deg yaw, 125 knots, 569 rpm.

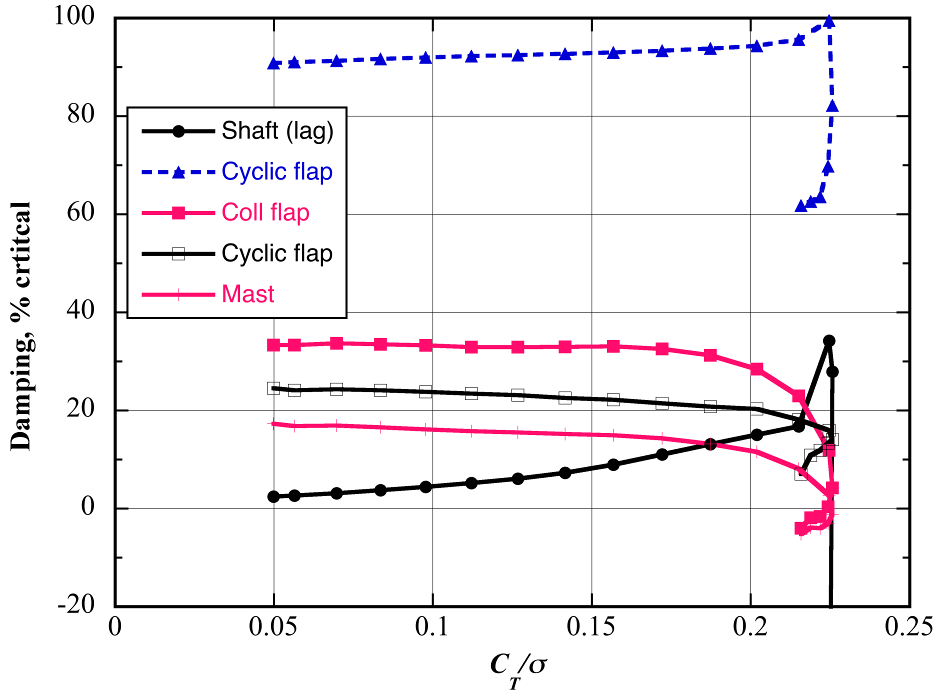

Fig. 8a. Predicted TTR/609 hover damping vs. thrust, 0-deg yaw, 569 rpm.

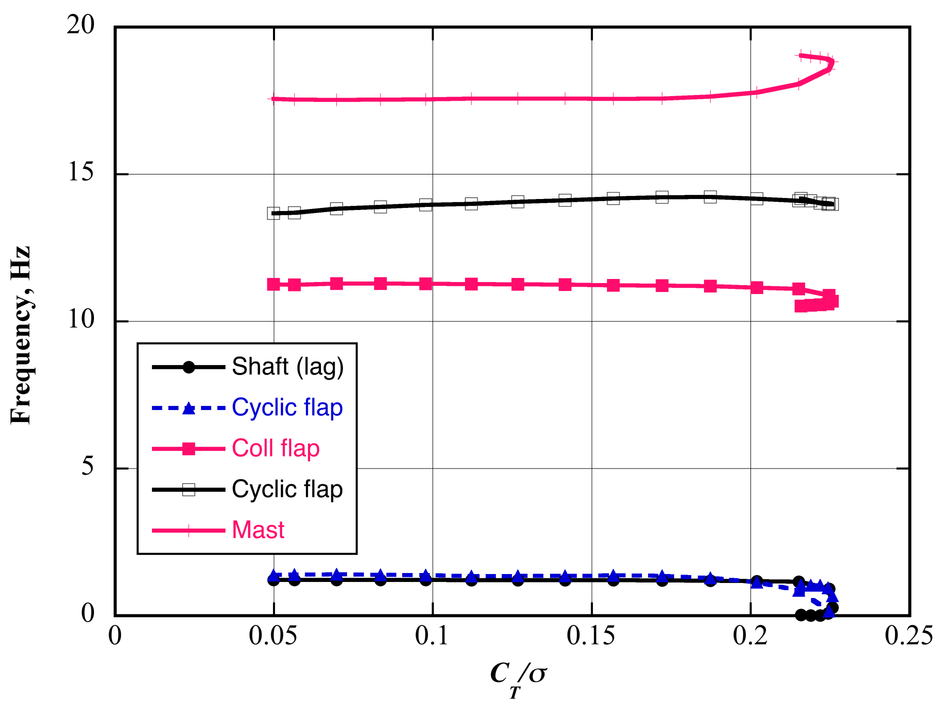

Fig. 8b. Predicted TTR/609 hover frequencies vs. thrust, 0-deg yaw, 569 rpm.

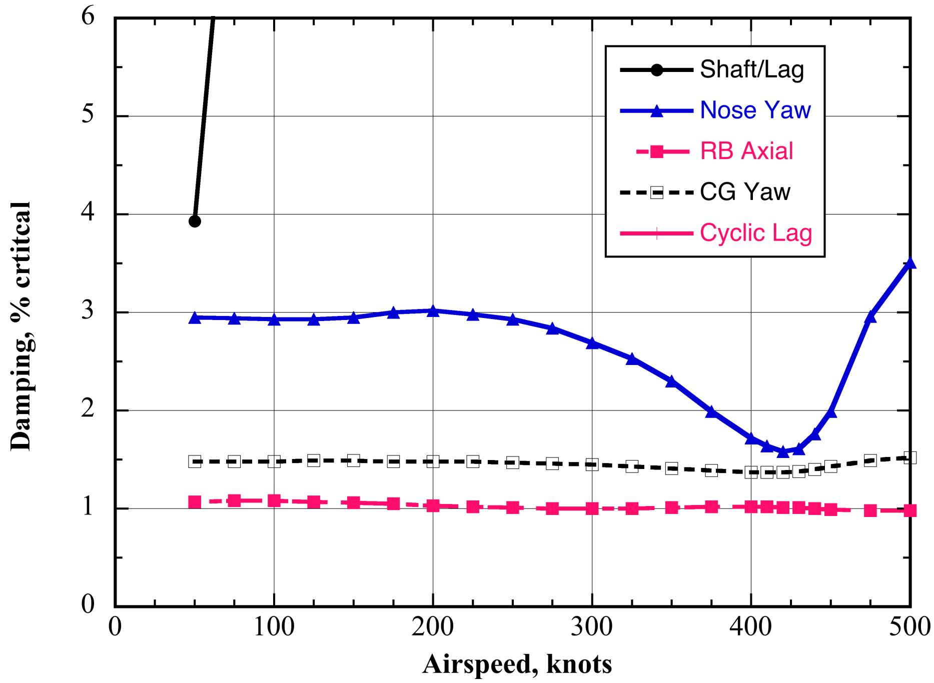

Fig. 9a. Predicted TTR/609 cruise (axial flow) damping vs. airspeed, 0-deg yaw, 0 power, 478 rpm.

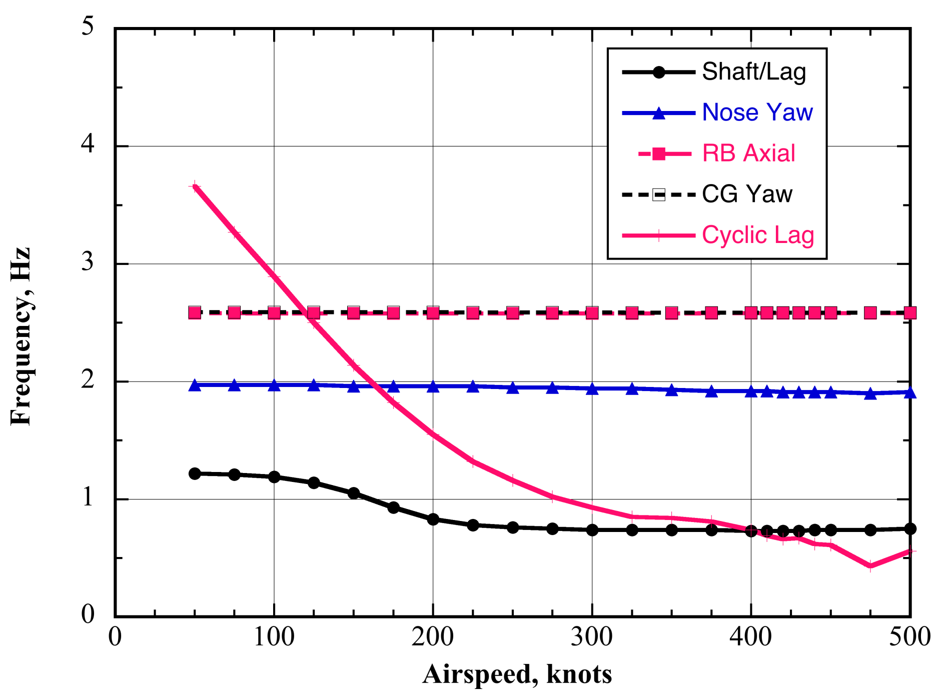

Fig. 9b. Predicted TTR/609 cruise (axial flow) frequencies vs. airspeed, 0-deg yaw, 0 power, 478 rpm.

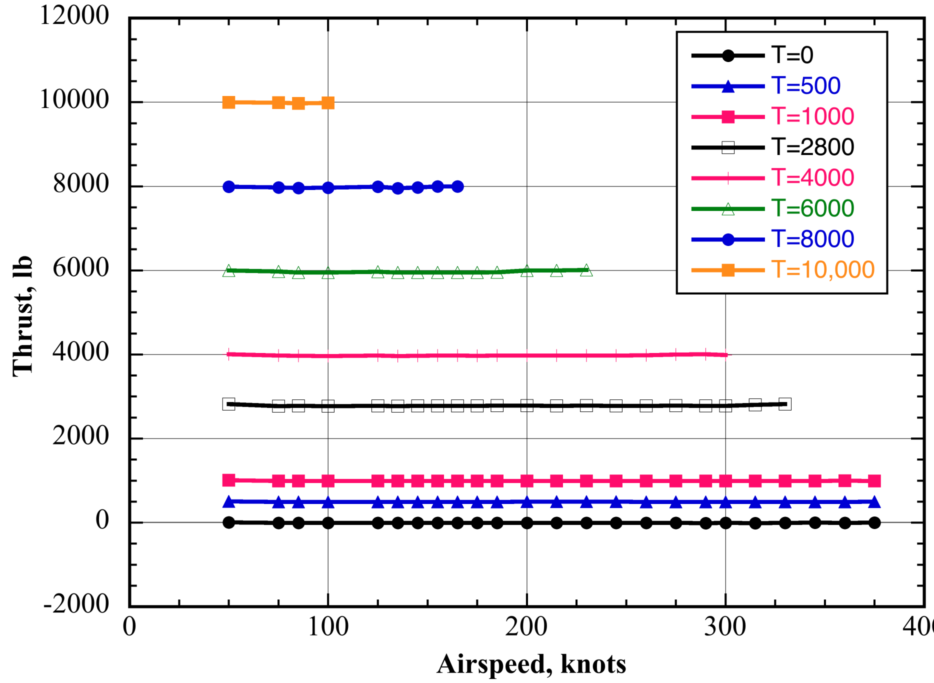

Fig. 10a. Predicted TTR/609 conversion (axial and edgewise flow) trim thrust vs. airspeed, 45-deg yaw, 569 rpm.

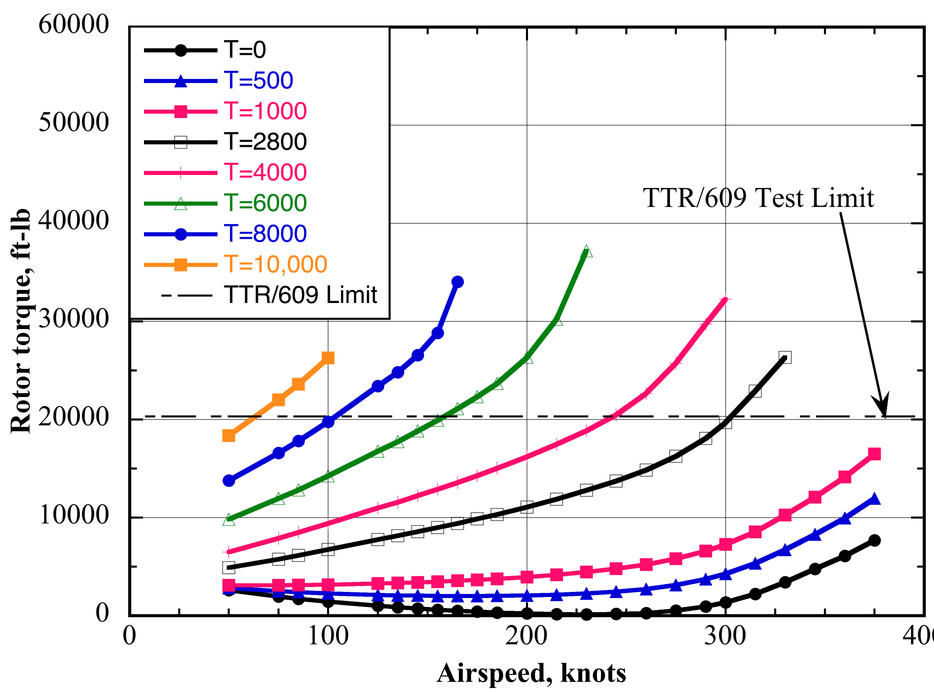

Fig. 10b. Predicted TTR/609 conversion (axial and edgewise flow) torque vs. airspeed, 45-deg yaw, 569 rpm.

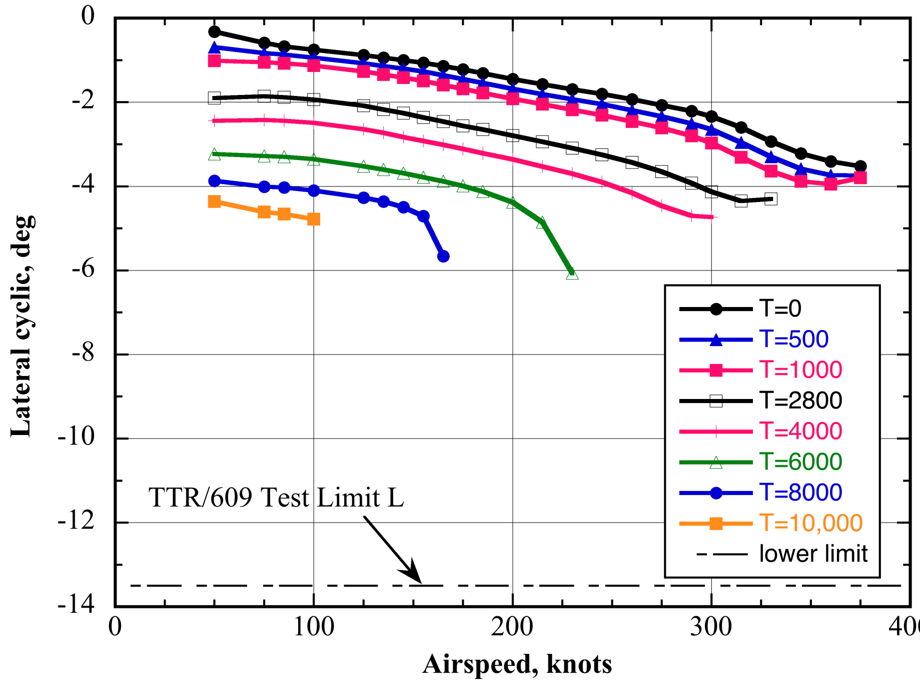

Fig. 10c. Predicted TTR/609 conversion (axial and edgewise flow) lateral cyclic vs. airspeed, 45-deg yaw, 569 rpm.

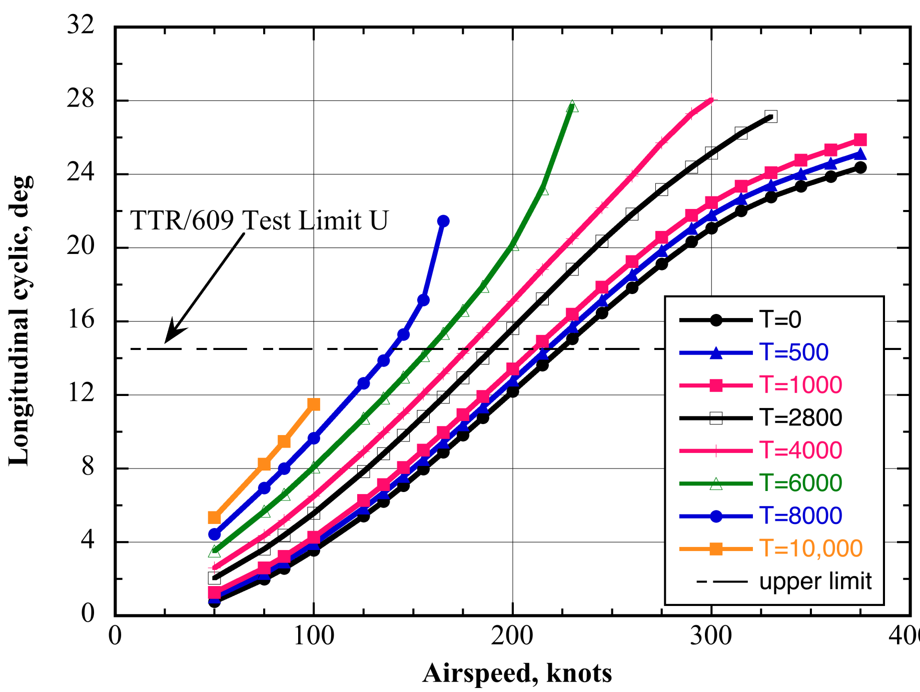

Fig. 10d. Predicted TTR/609 conversion (axial and edgewise flow) longitudinal cyclic vs. airspeed, 45-deg yaw, 569 rpm.

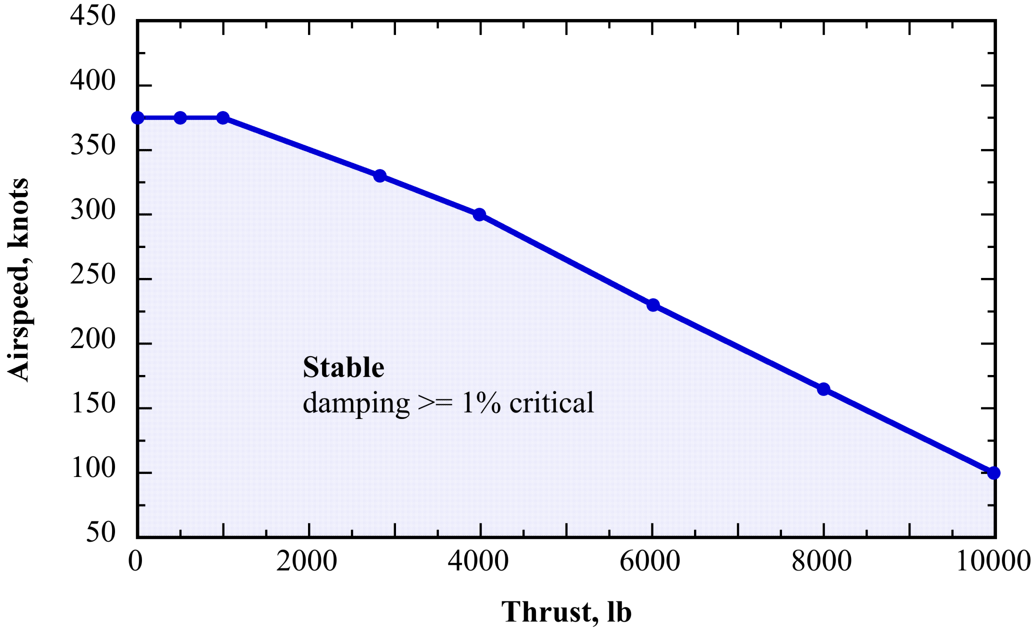

Fig. 10e. Predicted TTR/609 conversion (axial and edgewise flow) 1% damping stability envelope, 45-deg yaw, 569 rpm (rap test modal data).

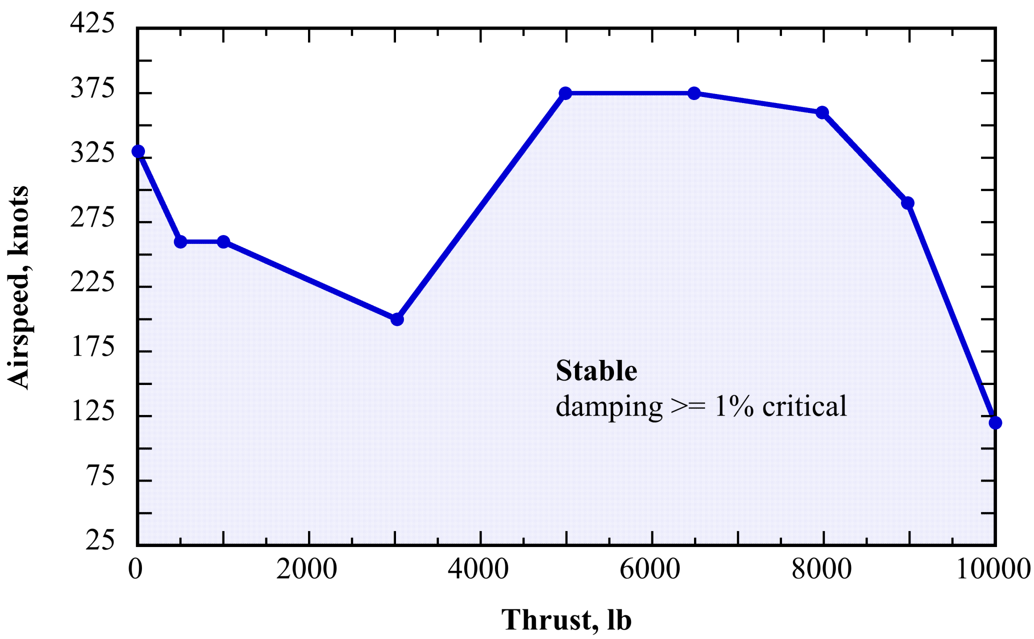

Fig. 11a. Predicted TTR/609 helicopter mode (axial and edgewise flow) 1% damping stability envelope, 90-deg yaw, 569 rpm (rap test modal data).

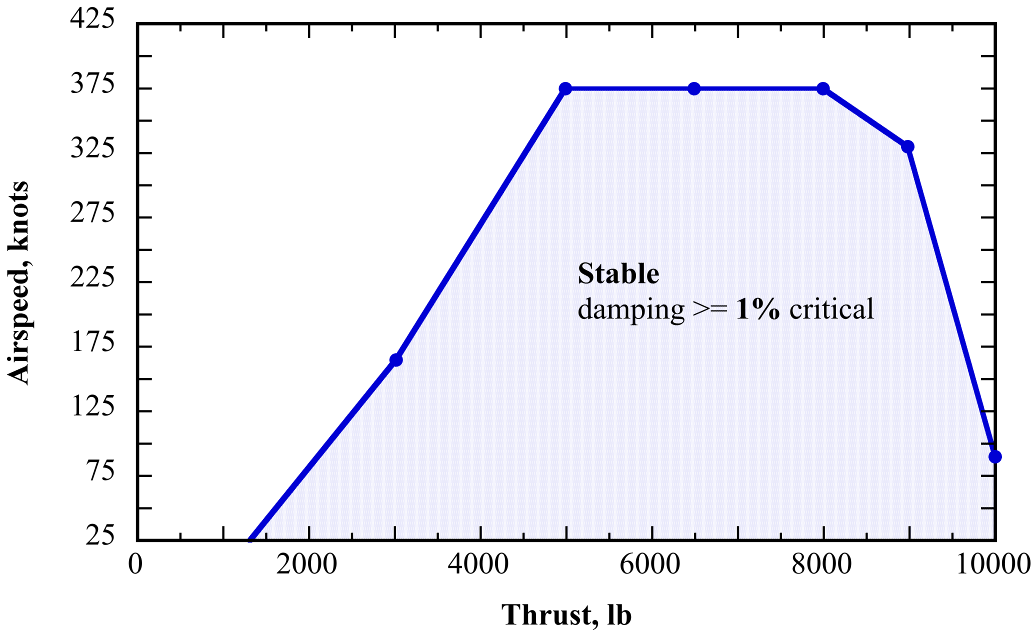

Fig. 11b. Predicted TTR/609 helicopter mode (axial and edgewise flow) 1% damping stability envelope, 90-deg yaw, 569 rpm (shake test modal data).

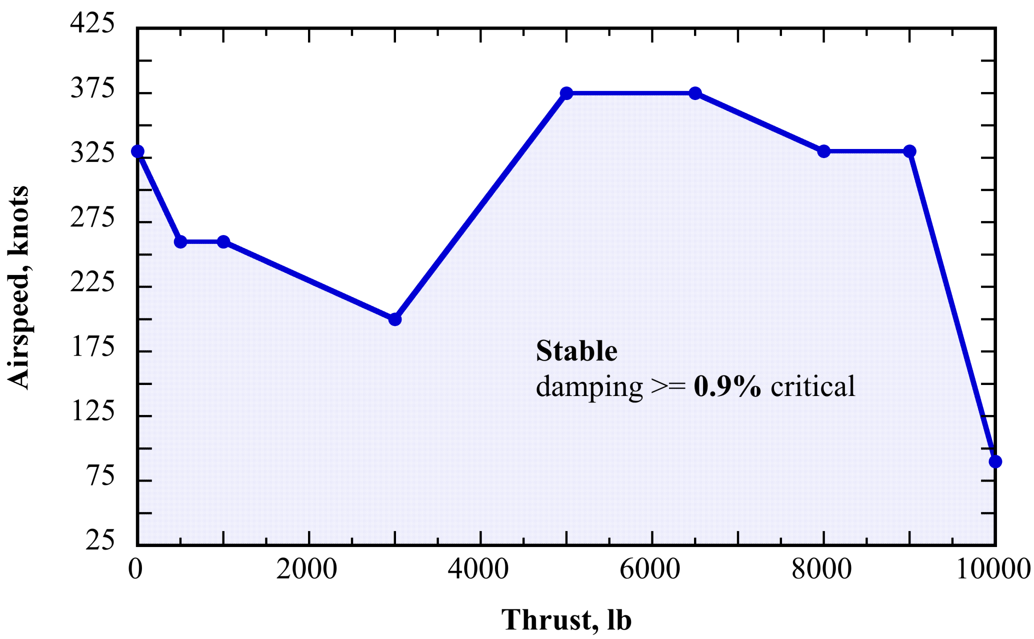

Fig. 11c. Predicted TTR/609 helicopter mode (axial and edgewise flow) 0.9% damping stability envelope, 90-deg yaw, 569 rpm (shake test modal data).